Supporting Information

Genini et al. 10.1073/pnas.1615730114

SI Materials and Methods

Cell Lines, Plasmids, Chemicals, and Antibodies. Cell lines (H358, DU145, LNCaP) were purchased from American Type Culture Collection (LGC Promochem, Molsheim Cedex, F) and maintained in RPMI supplemented with 10% FBS. Immortalized prostate epithelial cells (LHS) and a Ras-transformed counterpart (LHS-Ras) were described previously (58). WT and STAT3-deficient immortalized MEFs were previously described (6) and maintained in DMEM supplemented with 10% FBS. Complete DMEM, RPMI, and glucose-free RPMI were purchased from PAA (Brunschwig) and Life Technology (LuBioScience), respectively. DU145 ρ° cells were produced by culturing cells in RPMI in presence of ethidium bromide (50 ng/mL), uridine (10 mg/mL), and sodium pyruvate (1 mM) (59). Full-length WT EGFP-STAT3 was provided by Nadya I. Tarasova, Georgetown University, Washington, DC, and full-length pDest-mCherry-p62 was provided by Terje Johansen, University of Tromsø, Tromsø, Norway. EGFP-STAT3 and Cherry-p62 mutants were generated by site-directed mutagenesis using GENEART Site-Directed mutagenesis (Life Technology).

The following chemicals were used: OPB-51602 and OPB-31121 (Otsuka Pharmaceuticals); STA-21 and 2-Deoxy-2-fluoro-D-glucose (Santa Cruz Biotechnology); cryptotanshinone (Merck); NVP-BSK805 (Novartis); Stattic, WP1066, Rotenone, CCCP, rapamycin, and sodium pyruvate (ENZO Life Sciences); Mito-Tracker Orange CMTMRos (Life Technologies); CDDO-Me, PS341, antimycin A, chloroquine, valinomycin, glucose, 2-DG, uridine, and ethidium bromide (Sigma-Aldrich Chemie). IL-6 was purchased from R&D Systems Europe. The following antibodies were used: STAT3, pTyr705, and pSer727 (Cell Signaling Technology); HDAC6 (Santa Cruz Biotechnology); Ubiquitin (ENZO); p62, LC3 (Sigma-Aldrich Chemie); tubulin (Merck KGaA); GAPDH (Millipore).

Immunoblotting. Cells were treated with drugs or vehicle (0.1% DMSO) in complete fresh RPMI, glucose-free RPMI, or conditioned medium (i.e., medium from 4-d-old high-density cultures). Cells were lysed in a low-detergent (LD) buffer containing 25 mM Tris·HCl pH 7.4, 150 mM KCl, 5 mM EDTA, 1% Nonidet P-40, 0.5% sodium deoxycholate, 0.1% SDS supplemented with protease and phosphatase inhibitor mixture (Roche Diagnostics). High-detergent (HD) lysis buffer contained 30% glycerol, 4% SDS, 4% 2-mercapto-ethanol, 20 mM Tris·HCl pH 6.8, and 0.2% bromophenol blue. Subcellular fractionation into cytoplasm (I), membrane/organelle fraction (II), nuclei (III), and cytoskeletal fraction (IV) was performed using *ProteoExtract* Subcellular Proteome Extraction Kit (Merck). To isolate cell fractions by sucrose gradient centrifugation, cells were lysed in 10 mM Tris·HCl, pH 8.0, 7.5 mM ammonium sulfate, 1 mM EDTA, 0.025% Nonidet P-40, and 1 mM DTT. After incubation on ice for 5 min, sucrose (0.3 M final concentration) was added to the cell homogenate and the cellular fractions were separated by centrifugation at 4,000 × *g* for 10 min at 4 °C. Mitochondria were separated from the cytosolic fraction by centrifugation at 12,000 × *g* for 30 min at 4 °C. Protein concentration was determined using a BCA assay (Pierce, Perbio Science Switzerland SA). Proteins were loaded on 10–12% Sprint Next Gel (Amresco, Bioconcept) and analyzed by immunoblotting. Horseradish peroxidase-conjugated secondary antibodies and the WesternBright ECL detection system (Witec AG) were used for detection.

Cell Viability, Clonogenicity, and Stem-Like Properties. For proliferation assays, DU145 and H358 cells were plated in 96-well plates in complete RPMI at 1,000–2,000 cells per well (low density) or 20,000–30,000 cells per well (high density). Cells were treated with indicated compounds or DMSO (0.1%) after 24 h and cell viability was assessed after 72 h with the MTT assay. Alternatively, cell number was determined using sulforhodamine B (Sigma) colorimetric assay. For clonal assay cells were plated in six-well plates and treated with the indicated compounds. Colonies were fixed, stained with 1% Crystal violet in 20% ethanol, and counted with an automated colony counter. Tumorsphere formation and assessment of stem-like subpopulation ($CD44^+/CD24^-$ cells) by flow cytometry were performed as described previously (37). All assays were performed in triplicate and repeated in at least three independent experiments. Results are represented as mean ± SD from three independent experiments.

Production and Purification of STAT3 SH2D. pGEX-2T-GST-STAT3 SH2D was generated by cloning the STAT3 SH2D (amino acid residues 586–685) recovered from pET28a-STAT3-SH2D (GenScript) using BamHI and EcoRI into pGEX-2T vector (GE Healthcare Europe). Mutants of the GST-STAT3 SH2D were produced by site-directed mutagenesis. *Escherichia coli* strain BL21(DE3) (Life Technologies) transformed with the pGEX-2T-GST-STAT3 SH2D plasmid was grown at 37 °C in LB medium containing ampicillin (50 μg/mL) and induced with 1 mM isfopropyl-β-D-thiogalactopyranoside (IPTG) for 4 h at 37 °C. The bacterial pellet was suspended in cold PBS containing protease inhibitors and 1 mg/mL of lysozyme (Sigma-Aldrich) and sonicated. Triton X-100 (Sigma-Aldrich) was then added at a final concentration of 1% and the lysate was centrifuged for 20 min at 4 °C. Supernatant was filtered and purified by affinity chromatography using GSTrap HP column (GE Healthcare). Fusion protein was eluted with 10 mM glutathione reduced, desalted in PBS and concentrated to 1 mg/mL.

ITC. ITC measurements of the SH2D and binding inhibitors were conducted with a Nano ITC (TA Instruments) at 25 °C (22). After temperature equilibration, OPB-51602 at 100 μM in 1% DMSO (vol/vol) was titrated (1-μL step) every 4 min in 10 μM of GST-SH2D solution in PBS containing 1% DMSO (vol/vol) and (GST-SH2 WT, GST-SH2S636A, or GST-SH2V637A mutants) containing cells under constant stirring. Heat of reaction was subtracted from blank [1% DMSO (vol/vol)] titrated in GST solution in PBS containing 1% DMSO (vol/vol). The ratio heat/Mole of injectant was plotted versus the Molar ratio. The enthalpy of reaction, ΔH^0, the binding constant, K, and the stoichiometry value, n, were calculated from the measured heat changes, upon association of the inhibitor with the GST-SH2D target protein.

Molecular Modeling. The crystal structures of STAT3 protein was obtained from the available PDB file in the Protein Data Bank repository, 1BG1 (60). All compound structures were designed and optimized using *Discovery Studio* (DS, v2.5, Accelrys Inc) (22). All docking experiments were performed with *Autodock* 4.4, with *Autodock Tools* 1.4.6 on a *win64* platform following a consolidated procedure. The binding free energy, ΔG_{bind}, between the drugs and STAT3 was estimated by using to an extensively validated procedure (22, 61) based on the MM/PBSA approach implemented in *Amber 12* (62). According to this computational recipe, ΔG_{bind} values are calculated for equilibrated structures extracted from the corresponding molecular dynamics (MD)

trajectories. The ΔG_{bind} was calculated for each molecular species (complex, receptor, and ligand), and the binding free energy was computed as the difference: $\Delta G_{bind} = G_{complex} - (G_{receptor} + G_{ligand}) = \Delta E_{MM} + \Delta G_{sol} - T\Delta S$, in which ΔE_{MM} represents the molecular mechanics energy, ΔG_{sol} includes the solvation free energy, and $T\Delta S$ is the conformational entropy upon ligand binding. The per residue binding free-energy decomposition was performed exploiting the MD trajectory of each inhibitor/STAT3 complex, with the aim of identifying the key residues involved in the ligand/receptor interaction. This analysis was carried out using the MM/GBSA approach (63), and was based on the same snapshots used in the binding free-energy calculation. All simulations were carried out using the Pmemd modules of *Amber 12*, running on own CPU/GPU calculation cluster.

Glucose Uptake, Mitochondrial Membrane Potential, and Autophagy. Cells were seeded in six-well plates for 48 h and then treated with the indicated compounds in fresh RPMI or glucose-free RPMI for 2 or 6 h. Cells were harvested by adding 2 mM EDTA, stained according the specific protocols, and analyzed with FACS Fortessa (BD Biosciences) and FlowJo software. To measure glucose uptake, cells were stained with 2-deoxy-2-[87-nitro-2,1,3-benzoxadiazol-4-yl)amino]-D-glucose (2NBDG, Life Technology). Mitochondria membrane potential was assesses with JC-1 or $DIOC_6$ (ENZO). Autophagy was monitored with Cyto-ID Autophagy DetectionKit (ENZO). Mitochondria were isolated with Mitochondria Isolation Kit according to the manufacturer's instructions (Thermo Scientifics).

Lactate and ATP Level. Lactate production was determined using the Lactate Assay Kit (Sigma-Aldrich Chemie) according to the manufacturer's instructions. Cells were seeded in six-well plates, grown for 48 h, and then medium was changed as indicated. Cells were suspended in Lactate Assay Buffer and homogenized. Lactate was detected after adding the Master Reaction Mix and incubating for 30 min at room temperature using the AD340 multiplate reader (Beckman Coulter). To assess intracellular ATP level, cells were seeded in 96-well plates and grown for 48 h. For analysis in glucose-free RPMI, medium was changed 4 h before treatment with the indicated drugs. At the end, CellTiter-Glo Reagent (Promega) was added and luminescence was recorded using a Veritas Microplate Luminometer (Turner Biosystem, Promega).

OCR. The OCR was measured using the Seahorse XFp Analyzer (Seahorse Bioscience) under standard conditions and after addition of 1 μM oligomycin, 0.5 μM FCCP, and 0.5 μM Rotenone/antimycin A (XFp Cell Mito Stress Test Kit) with or without pretreatment with OPB-51602 (100 nM), according to the manufacturer's instructions. DU145 cells were seeded in the XFp miniplates and grown overnight. Test compounds were diluted in XF Base Medium containing 1 mM pyruvate, 2 mM glutamine, and 10 mM glucose at pH 7.4, and were sequentially injected. OCR (picomoles per minute) was measured in basal condition and after injection of OPB-51602 and each test compound.

Immunoprecipitation. Cells were fractioned using ProteoExtract Subcellular Proteome Extraction Kit and lysates subject to immunoprecipitation (IP). Alternatively, IP was performed by lysing cells on ice in DISK IP lysis buffer (30 mM Tris, pH 7.5, 150 mM NaCl, 10% glycerol, 1% Triton X-100). Cell lysates were cleared twice by centrifugation at 4 °C at maximum speed. IP was performed using anti-STAT3 antibody at 4 °C. Immunocomplexes were then recovered by PureProteome Protein A+G Magnetic Beads (Millipore), washed with DISK buffer, and eluted using HD buffer.

RNA Interference. Cells were seeded at 30–50% confluence and transfected with 20 nM siRNA (Ambion, Applied Biosystems) directed to p62 (sip62) and firefly luciferase (siGL3) using Interferin (Polyplus, Brunschwig). After 48 h, cells were treated with OPB-51602 for 16 h and then analyzed by Western blotting. Alternatively, cells transfected with EGFP-STAT3 were treated with OPB-51602 for 4 h and analyzed by confocal microscopy. For STAT3 knockdown, cells were transfected with 100 nM siRNA using Lipofectamine 2000 (Sigma). Cells were analyzed by immunoblotting and flow cytometry after 72 h.

Fluorescence Microscopy. Cells were incubated with drugs in fresh, glucose-FM or CM as indicated for Western blot analysis. Cells were seeded in eight-well Millicell EZ SLIDE (Millipore) to reach 80% confluence on the next day. Cells were transfected with EGFP-STAT3 and pDest-mCherry-p62 or the mutants using jetPRIME (Polyplus, Brunschwig). After 48 h, cells were treated with the drugs for 6 h, then fixed with 4% paraformaldehyde, and mounted with VECTASHIELD Mounting Medium with DAPI (Reactolab). MitoTracker Orange was added to culture medium for 40 min. Cells were washed once with PBS, fixed with 4% paraformaldehyde, and mounted with VECTASHIELD Mounting Medium. Confocal sections were obtained with a Leica TCS SP2 AOBS confocal laser microscope by sequential scanning. p62 aggregates were detected in 3-μm sections from formalin-fixed paraffin-embedded xenografts mounted on positive-charged slides. Slides were de-paraffinized with xylene and rehydrated; endogenous peroxidase activity was blocked by 3% hydrogen peroxide solution. The antigen retrieval was induced by heating the slides in EDTA pH8, boiling, followed by 20 min at sub-boiling temperature. Nonspecific binding sites were blocked with 5% BSA in PBS. Histological sections were incubated overnight at 4 °C with primary antibodies p62 and E-cadherin followed by secondary antibodies Alexa Fluor-594 goat anti-rabbit IgG and Alexa Fluor-488 goat anti-mouse IgG, respectively. Cell nuclei were counterstained with DAPI. Five-micrometer sections were stained to detect aggresomes using the ProteoStat Aggresome detection kit (ENZO). Slides were de-paraffinized with xylene and rehydrated, subsequently washed with PBS 1×, and fixed in 10% paraformaldehyde in PBS for 30 min at room temperature. Antigen retrieval was performed as described above. Sections were washed with PBS 1× and stained with ProteoStat dye, according to the manufacturer's instructions. p62 aggregates and aggresomes were counted using the Object-Counter3D plug-in of ImageJ software. From 200 to 800 cells per sample were analyzed. A threshold value was used to distinguish individual p62 aggregates (from 0.5-μm^2 area size) or aggresomes (from 0.1-μm^2 area size). Live imaging was done on a Cytation3 Imaging Reader (Biotek Instruments) and green cells were automatically counted by the Gen5 Image software. Additionally, live fluorescence imaging was performed on the BD Pathway 855 confocal microscope (BD Biosciences).

RT-PCR. Cells were plated in T-25 flasks and treated with OPB-51602. Total RNA was purified with SV Total RNA Isolation System (Promega). RNA concentration was determined using a NanoDrop spectrophotometer (Witec AG). RT-PCR was performed using the SuperScript III One-Step RT-PCR System (Life Technology). PCR products were run on 2% agarose gels, stained with GelRed Nucleic Acid Stain (Brunschwig), and visualized using the AlphaImager 3400.

Reporter Assays. Cells expressing stable luciferase STAT3 reporter vector were plated in 48-well plates and treated with the drug (33). A single luciferase reporter assay was performed according to the manufacturer's instructions (Promega) using a Cytation3 Imaging Reader. Data were normalized for protein concentration.

Tumor Xenografts. Athymic male nude mice were purchased from Harlan Laboratories. Protocols were approved by the Swiss Veterinary Authority and conducted in compliance to the national guidelines. Experimental groups consisted of animals with equal age and body weight. To generate tumor xenografts, DU145 cells constitutively expressing luciferase (DU145-Luc) were injected subcutaneously. DU145-Luc cells were generated by infecting the cells with the retroviral vector pMMP-LucNeo, which encodes a fusion of the firefly luciferase and neomycin gene, and selection with 2 mg/mL G418 (Brunschwig). Pools of neomycin-resistant cells were collected and used for the experiments. Mice bearing subcutaneous tumors >100-mm^3 volume were treated with OPB-51602 (20–40 mg/kg in 5% arabic gum for 5 d/wk) or vehicle. Tumor size was measured with a caliper and by in vivo bioluminescence imaging after 2 wk of treatment using IVIS Spectrum Imaging System (Caliper LifeSciences, PerkinElmer). Data were analyzed using the Living Image software 4.2 (Caliper LifeSciences). Data represent mean ± SD of five mice per group. Animals were killed at the indicated time points. Tumor tissue was fixed and examined by IHC with the indicated antibodies using Histostain-Plus Invitrogen II Generation LAB-SA (Cat. no. 85–9043) Detection System Kit. Ex vivo assays to assess stem-like cancer cells in tumor tissues were performed as described previously (36, 37).

Statistical Analysis. Differences between experimental groups were analyzed for statistical significance using an unpaired two-tailed *t* test. *P* values ≤ 0.01 were considered statistically significant.

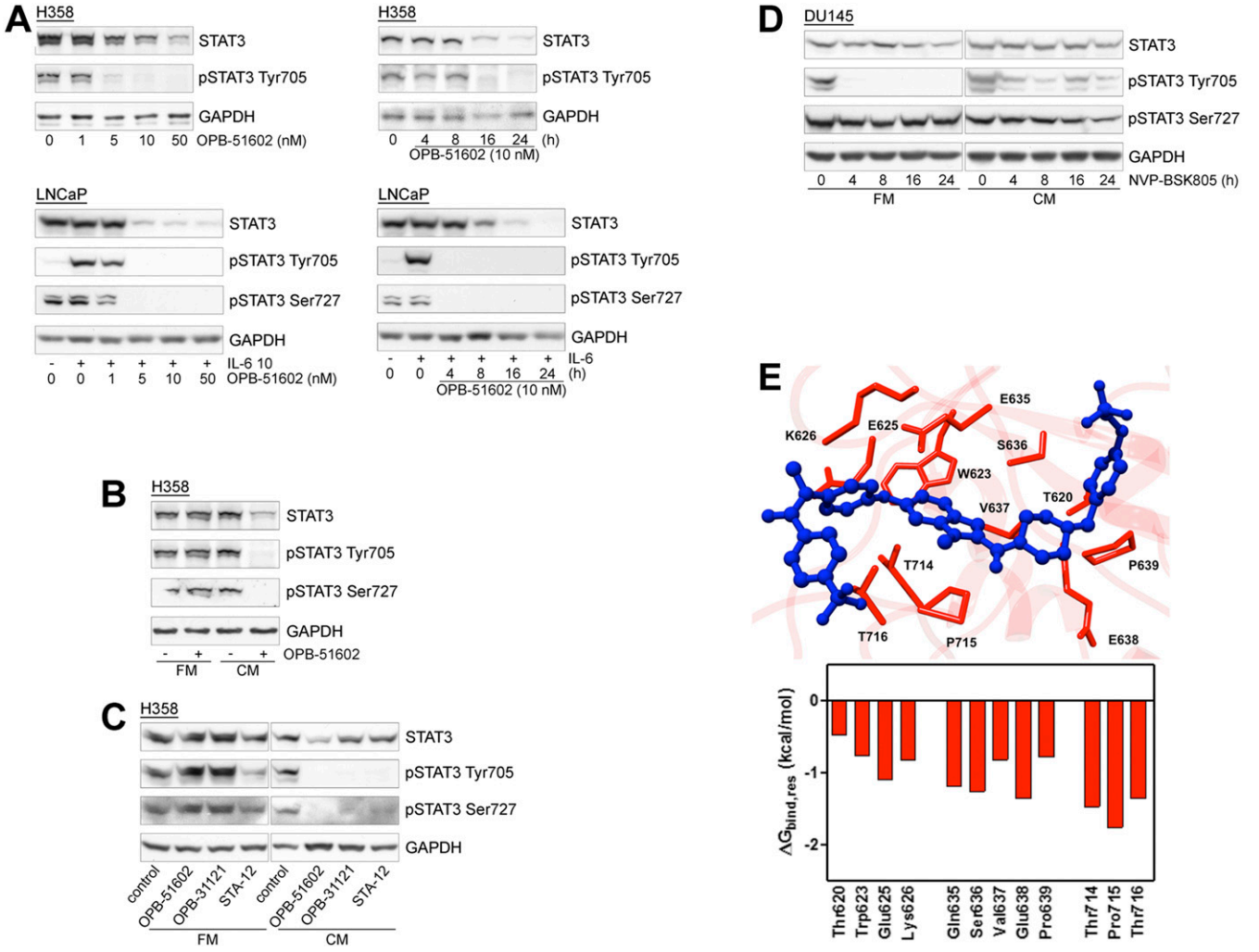

Fig. S1. OPB-51602 interferes with STAT3 signaling in cancer cells. (*A*) Immunoblot analysis of STAT3 and pSTAT3 in H358 and LNCaP cells treated with OPB-51602. (*B* and *C*) STAT3 and pSTAT3 in H358 cells treated with OPB-51602 and the indicated compounds for 16 h in FM or CM. (*D*) STAT3 and pSTAT3 in DU145 cells treated with NVP-BSK805 for 16 h in FM or CM. (*E*) Amino acids (red) in the OPB-51602 (blue) binding site in the STAT3 SH2D (*Upper*) and per residue energy decomposition analysis (*Lower*) of the complex.

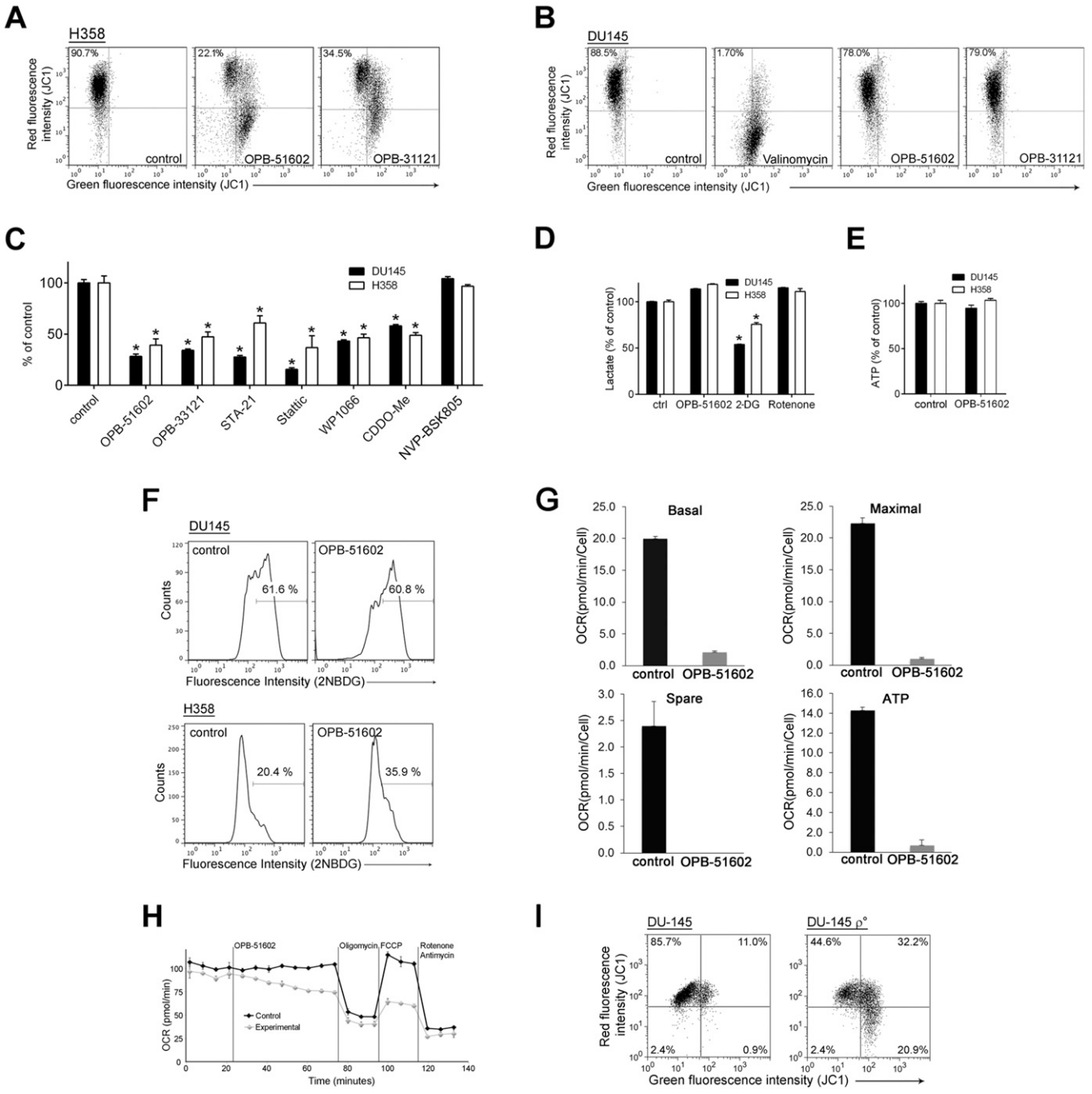

Fig. S2. OPB-51602 affects mitochondrial function. (*A*) MMP (JC1 staining) in H358 cells treated with OPB-51602 and OPB-31121 for 2 h in CM. (*B*) MMP (JC1 staining) in DU145 cells treated with OPB-51602, OPB-31121 and Valinomycin in FM. (*C*) ATP level in cells treated with the indicated drugs for 2 h in CM. (*D*) Lactate production in DU145 and H358 cells treated with OPB-5602, 2-DG (5 mM), and rotenone (10 μM) in FM. (*E*) ATP production in DU145 and H358 cells treated with OPB-51602 in FM. (*F*) Glucose uptake in DU145 and H358 cells treated with OPB-51602 for 6 h in FM. (*G*) Mitochondrial respiratory capacity and ATP production determined in control and OPB-51602 treated (100 nM for 2 h) DU145 cells by OCR measurement with Seahorse analysis shown in Fig. 2*B*. (*H*) Seahorse analysis of OCR of DU145 cells untreated (control) or treated (experimental) with OPB-51602 (100 nM) at the indicated time. (*I*) MMP (JC1 staining) in DU145 and DU-145 ρ° cells. $*P < 0.01$.

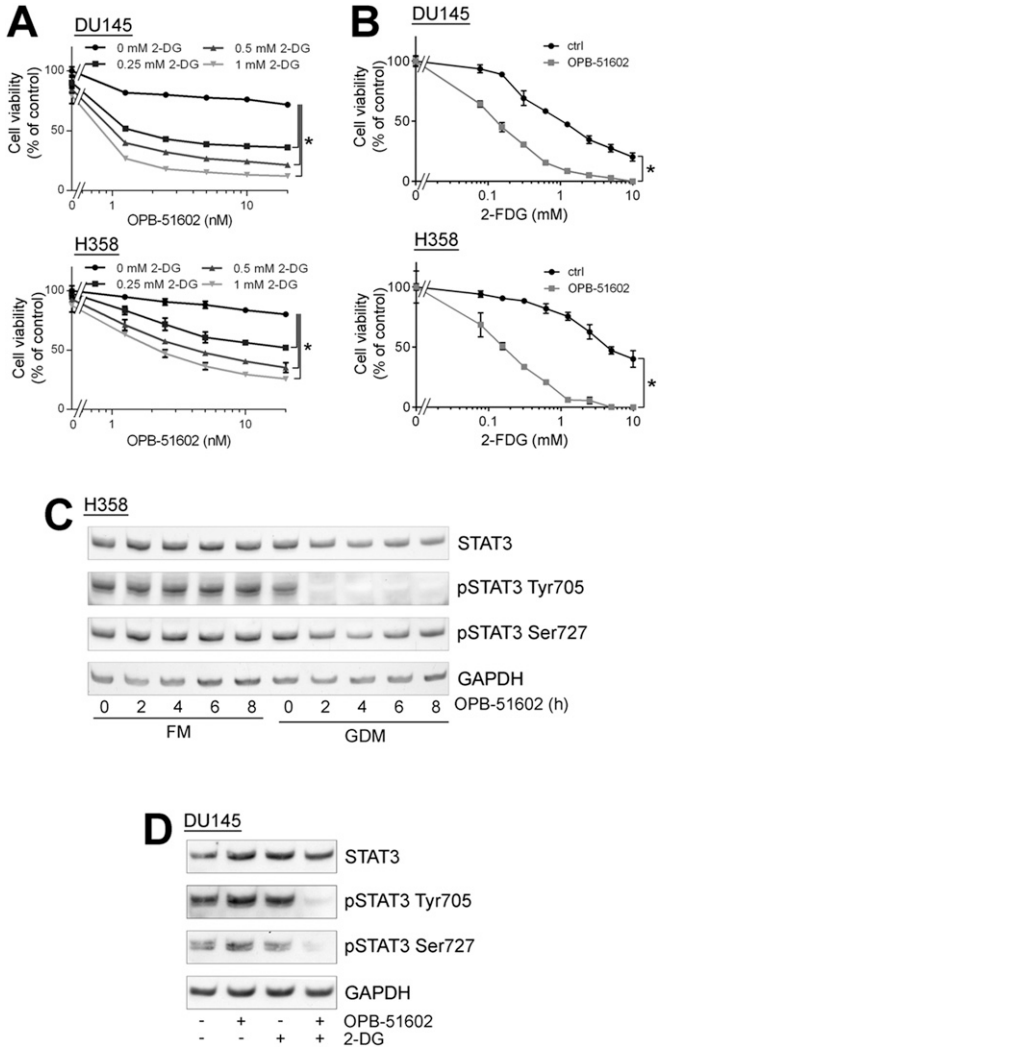

Fig. S3. Glucose starvation enhances the cellular response to OPB-51602. (*A* and *B*) Proliferation of DU145 and H358 cells treated with OPB-51602 in the presence of 2-DG (*A*) or 2-FDG (*B*). (*C*) STAT3 and pSTAT3 in H358 cells treated with OPB-51602 in FM or glucose-depleted FM (GDM). (*D*) STAT3 and pSTAT3 in DU145 cells treated with OPB-51602 and/or 2-DG (5 mM) for 4 h in FM.

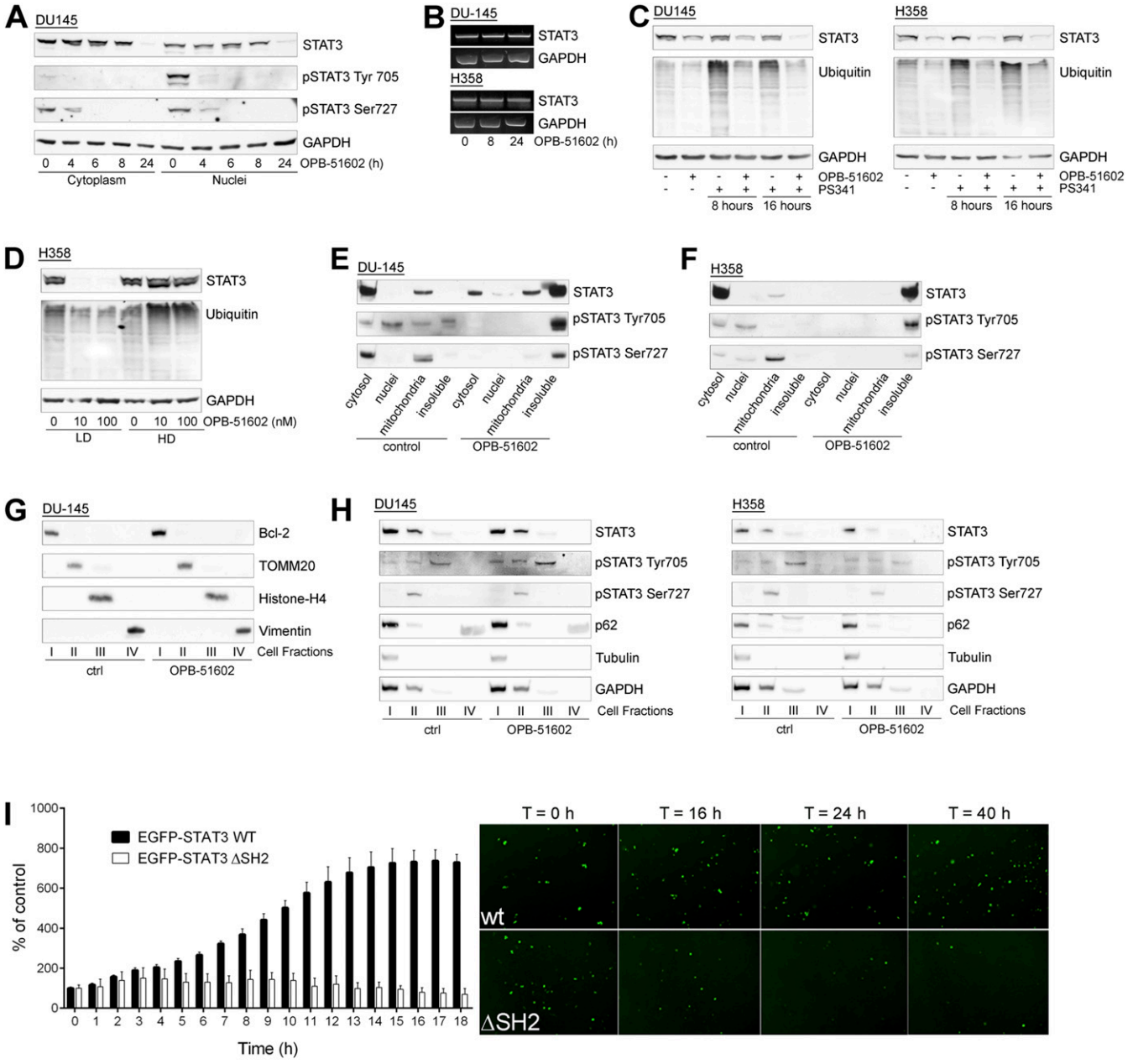

Fig. S4. Intracellular distribution of STAT3 after treatment with OPB-51602. (*A*) STAT3 and pSTAT3 distribution in cytoplasm and nuclei of DU145 cells untreated or treated with OPB-51602 in CM for the indicated time. (*B*) STAT3 mRNA in DU145 and H358 cells treated with OPB-51602 in CM. (*C*) STAT3 and ubiquitinated proteins in DU145 and H358 cells treated with OPB-51602 and PS-341 (10 μM) for the indicated time. (*D*) STAT3 and ubiquitinated proteins in control and OPB-51602–treated H358 cells lysed in low (LD) or high (HD) detergent buffer. (*E* and *F*), Cell fractionation by sucrose gradient centrifugation and analysis of intracellular distribution of STAT3 and pSTAT3 in control and OPB-51602 treated DU145 (*E*) and H358 (*F*) cells in CM. (*G*) Distribution of specific cell compartment markers after cell fractionation of control and OPB-51602–treated DU145 cells. (*H*) Intracellular distribution of STAT3, pSTAT3, and p62 in DU145 and H358 cells untreated or treated with OPB-51602 for 16 h in FM. (*I*) Time-lapse fluorescence microscopy determination of the percentage of viable WT and ΔSH2 EGFP-STAT3^{+} H358 cells and representative images at the indicated time posttransfection. (Magnification: 5×.)

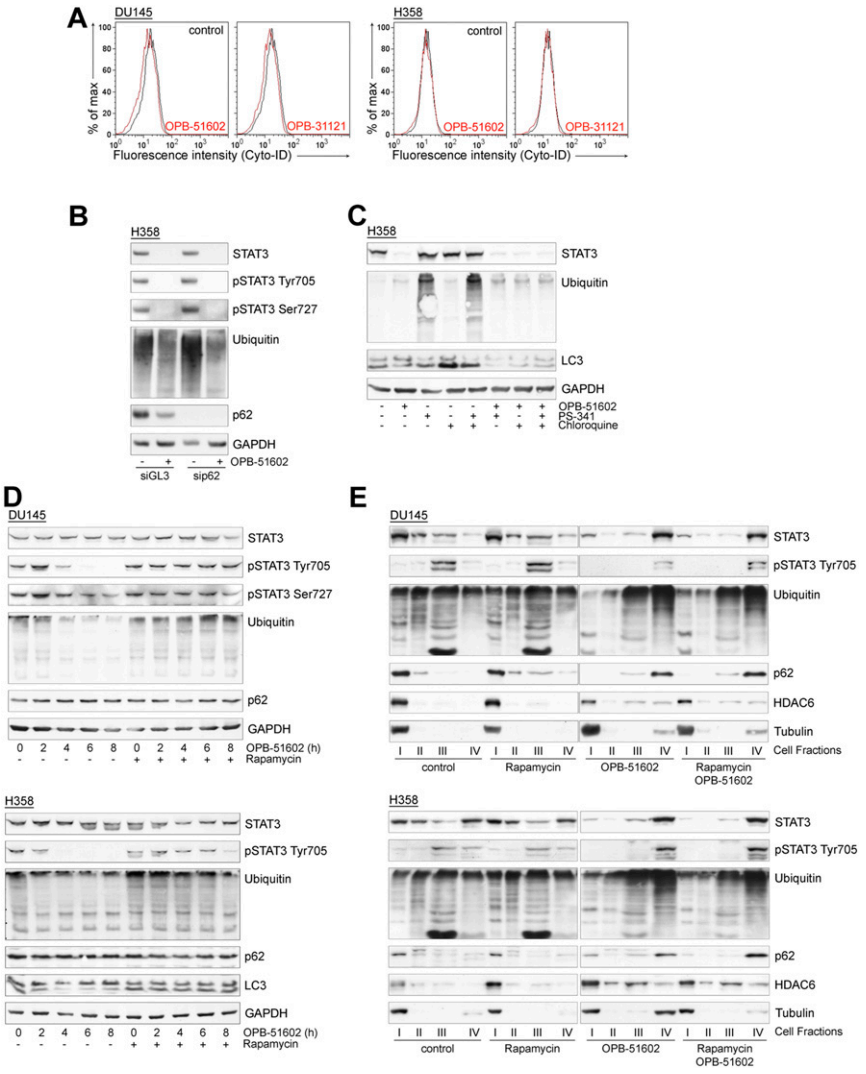

Fig. S5. OPB-51602 affects autophagy in glucose-starved cancer cells. (*A*) Immunoblot analysis of STAT3, pSTAT3, p62, and ubiquitinated proteins in control (siGL3) and p62 knockdown (sip62) cells with and without treatment with OPB-51602 for 16 h in CM. (*B*) Flow-cytometry analysis of autophagy in DU145 and H358 cells treated with OPB-51602 and OPB-31121 for 6 h in glucose-rich FM. (*C*) LC3, STAT3, and ubiquitinated proteins in H358 cells treated with OPB-51602, PS-341 (10 μM), and chloroquine (100 μM) for 16 h in CM. (*D*) STAT3, p62, and ubiquitinated proteins in DU145 (*Upper*) H358 (*Lower*) cells treated with OPB-51602 with or without rapamycin (1 μM) for up to 8 h in CM. (*E*) Distribution of STAT3 and the indicated proteins in DU145 (*Upper*) and H358 (*Lower*) cells treated with OPB-51602 and/or rapamycin (1 μM) for 16 h in CM.

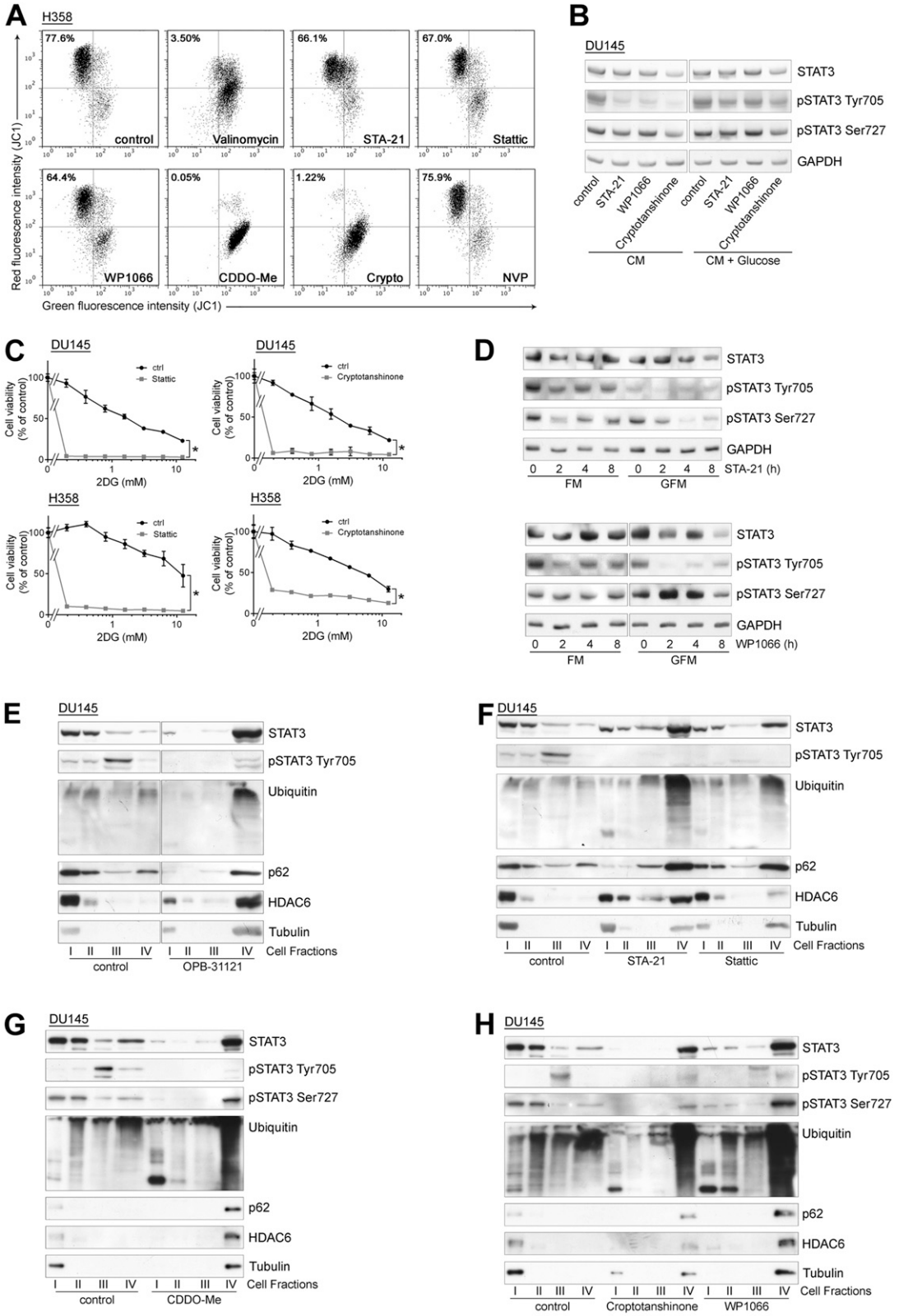

Fig. S6. Mitochondrial dysfunction and STAT3 redistribution in cells treated with STAT3 inhibitors. (*A*) MMP (JC1 staining) in H358 cells treated with Valinomycin (positive control) and the indicated STAT3 inhibitors in CM. (*B*) STAT3 and pSTAT3 in DU145 cells treated with STA-21 (50 μM), WP1066 (50 μM), and cryptotanshinone (10 μM) in CM and glucose-supplemented CM. (*C*) Proliferation of DU145 and H358 cells treated with Stattic or cryptotanshinone alone or in the presence of 2-DG. $*P < 0.01$. (*D*) STAT3 and pSTAT3 in DU145 cells treated with STA-21 (*Upper*) and WP1066 (*Lower*) in FM or glucose-FM (GFM). (*E–H*), Intracellular distribution of the indicated proteins in DU145 cells treated with OPB-31121 (*E*), STA-21 and Stattic (*F*), CDDO-Me (*G*), cryptotanshinone and WP1066 (*H*) in CM.

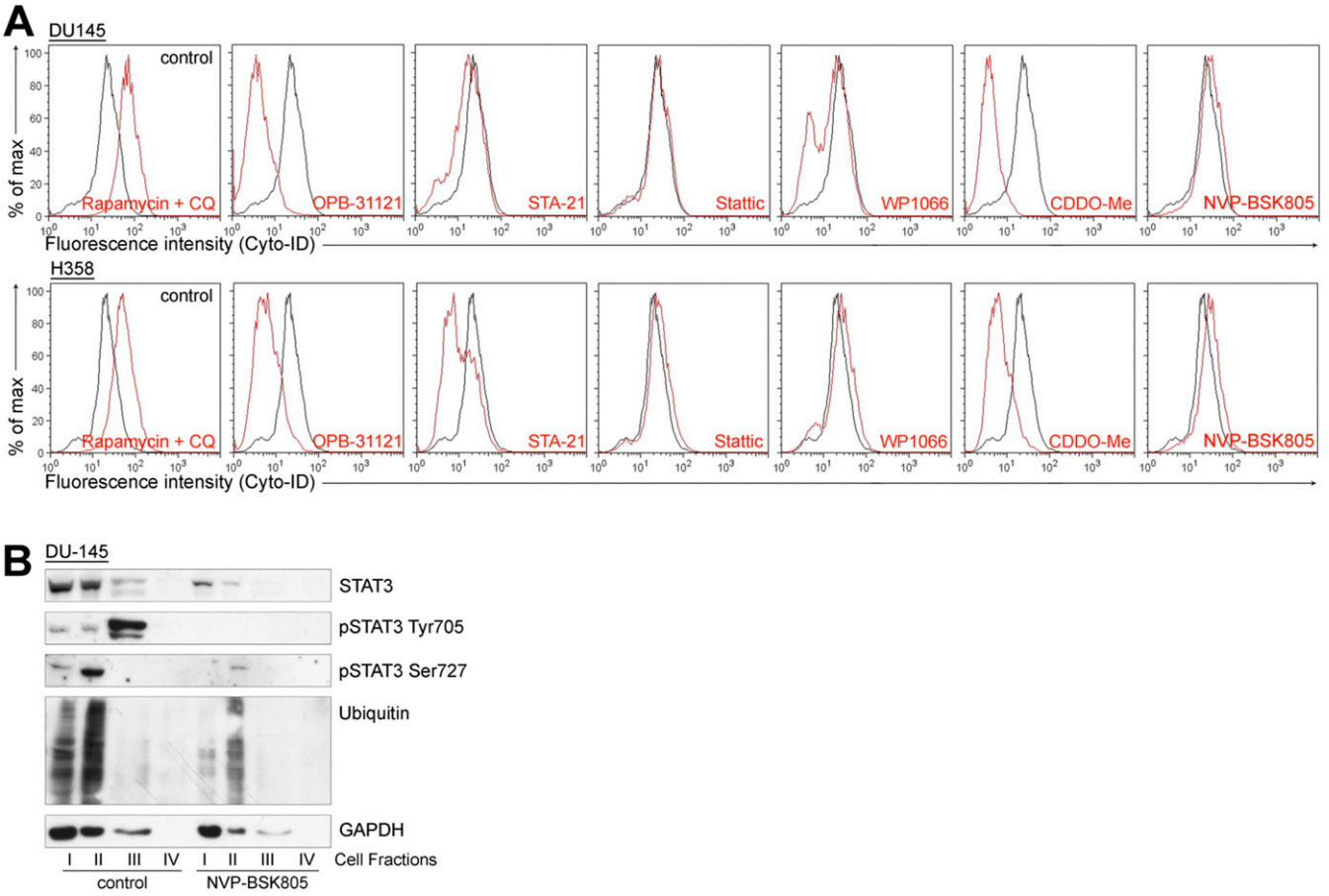

Fig. S7. Diverse impact on autophagy in response to STAT3 and JAK inhibitors. (*A*) Flow cytometry analysis of autophagy in DU145 and H358 cells treated with the indicated STAT3 inhibitors for 6 h in CM. (*B*) Distribution of STAT3 and pSTAT3 in DU145 cells treated with NVP-BSK805 for 16 h.

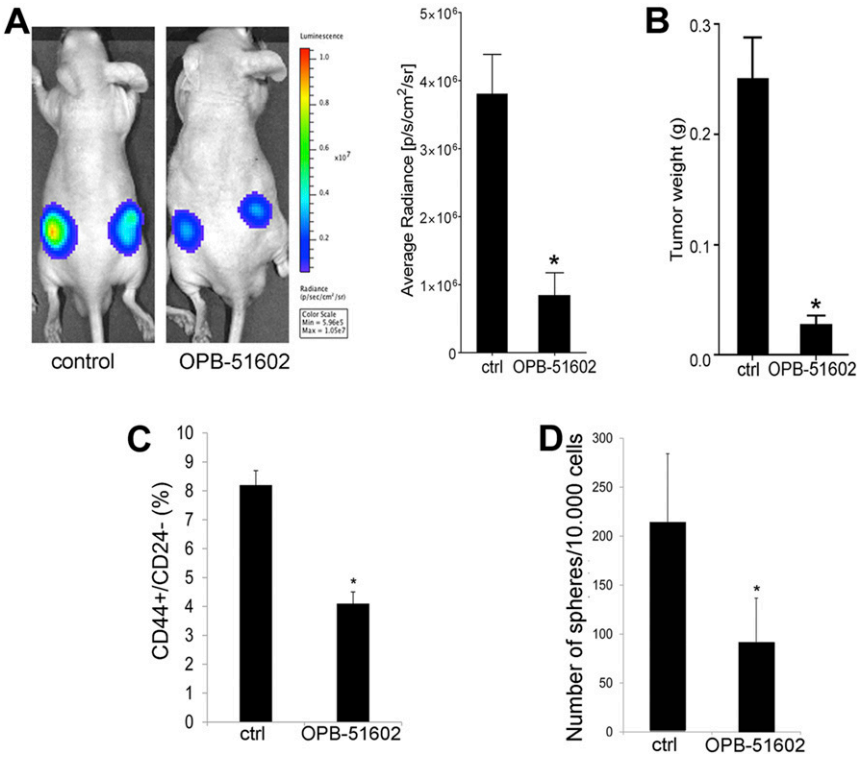

Fig. S8. In vivo activity of OPB-51602 in mouse tumor xenografts. (*A*) Tumor growth assessed in control and OPB-51602 treated animals by in vivo bioluminescence imaging after 2 wk of treatment. (*B*) Tumor weight assessed in control and OPB-51602 treated animals after 2 wk of treatment. (*C* and *D*) Fraction of $CD44^{+}/CD24^{-}$ cells (*C*) and ex vivo tumor-sphere forming ability (*D*) in cells isolated from control and OPB-51602 treated tumor xenografts after 2 wk of treatment (40 mg/kg, daily by mouth). $*P < 0.01$.

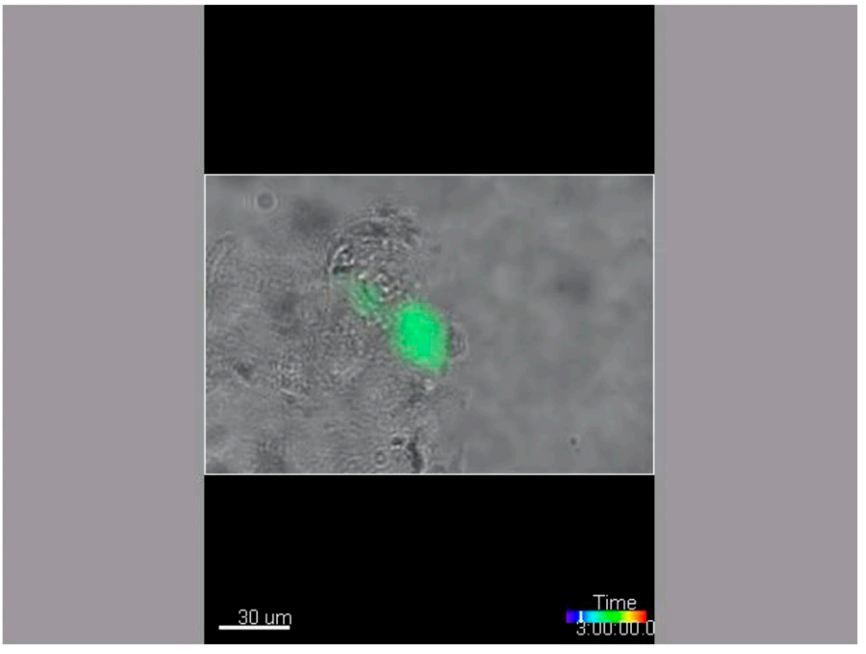

Movie S1. Live fluorescence microscopy analysis of H358 cells expressing WT EGFP-STAT3. Representative images of live cells in control sample (Exp. 1).

Movie S1

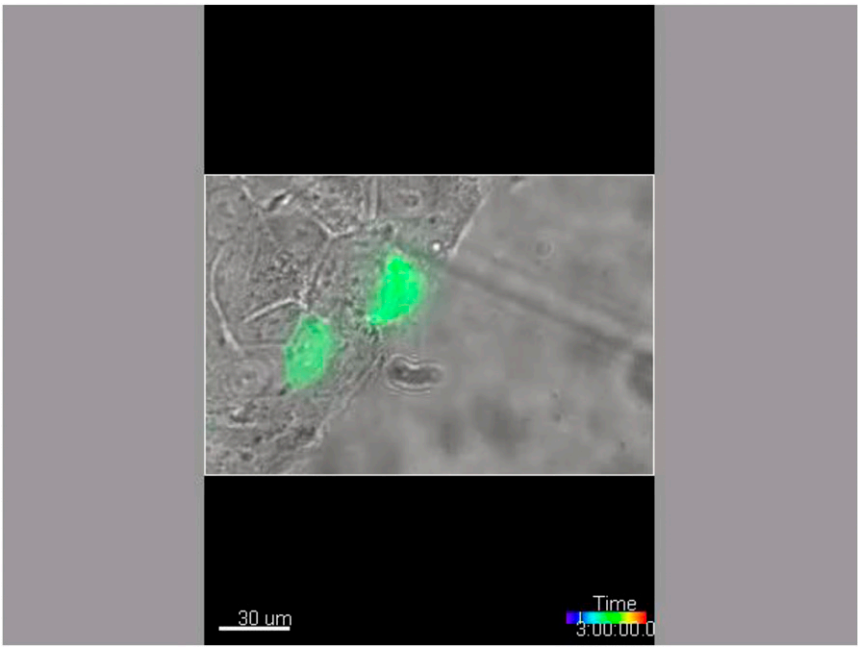

Movie S2. Live fluorescence microscopy analysis of H358 cells expressing WT EGFP-STAT3. Representative images of live cells in control sample (Exp. 2).

Movie S2

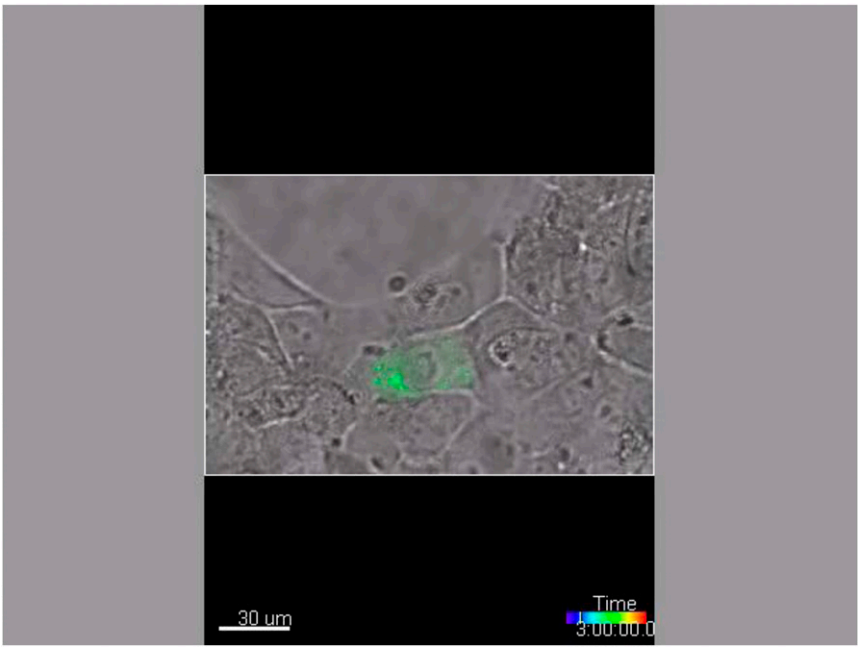

Movie S3. Live fluorescence microscopy analysis of H358 cells expressing ΔSH2 EGFP-STAT3. Representative images of cells expressing the self-aggregating STAT3 mutant undergoing proteotoxic cell death (Exp. 1).

Movie S3

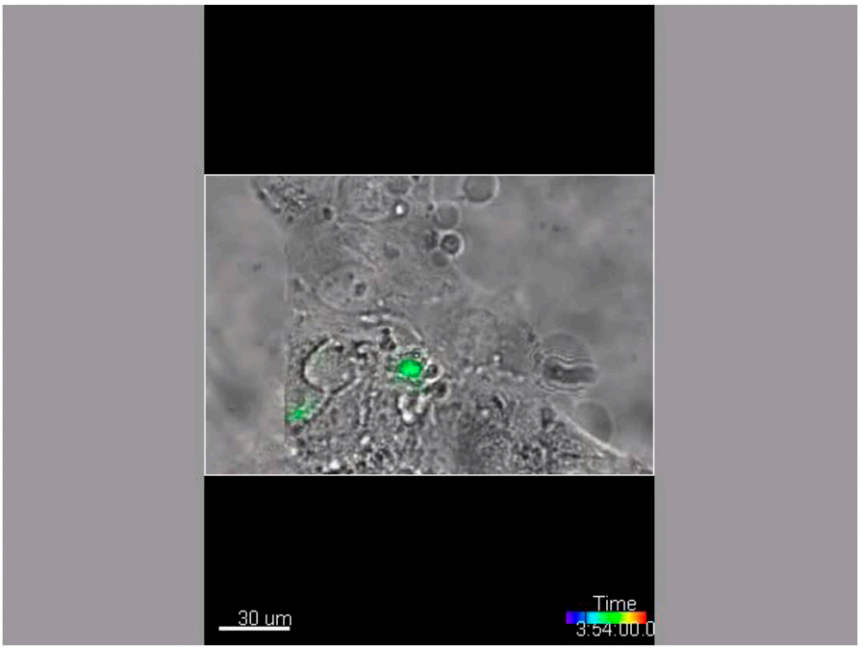

Movie S4. Live fluorescence microscopy analysis of H358 cells expressing ΔSH2 EGFP-STAT3. Representative images of cells expressing the self-aggregating STAT3 mutant undergoing proteotoxic cell death (Exp. 2).

Movie S4